Two-dimensional spectroscopic observation of a pulse-modulated induction thermal plasma torch for nanopowder synthesis

	Kodama Naoto, Kita K., Tanaka Yasunori, Uesugi Yoshihiko, Ishijima Tatsuo, Watanabe Shu, Nakamura Keitaro
journal or publication title	Journal of Physics: Conference Series
volume	550
number	1
page range	012026
year	2014-01-01
URL	http://hdl.handle.net/2297/40611

Two-dimensional spectroscopic observation of a pulse-modulated induction thermal plasma torch for nanopowder synthesis

N Kodama, K Kita, Y Tanaka, Y Uesugi, T Ishijima, S Watanabe†, K Nakamura†

Faculty of Electrical and Computer Engineering, Kanazawa University, Kakuma, Kanazawa 920-1192, JAPAN

†Research Center for Production & Technology, Nisshin Seifun Group Inc., 5-3-1 Tsurugaoka, Fujimino 356-8511, JAPAN

E-mail: `n_kodama@stu.kanazawa-u.ac.jp`, `tanaka@ec.t.kanazawa-u.ac.jp`

Abstract. The two-dimensional distributions of spectral radiation intensities in the plasma torch were observed for the pulse modulated induction thermal plasmas (PMITP) with continuous or intermittent feedstock feeding for TiO_2 nanopowder synthesis. For this observation, an imaging spectrophotometer with a high speed video camera were adopted. The evaporation of feedstock Ti powder, the formation of TiO and TiO transportation were investigated from the observation results of a Ti atomic spectral line and TiO molecule spectra as well as those of Ar and O atomic lines. An interpretation was suggested from the observation results for Ti feedstock evaporation and TiO formation in nanoparticle synthesis using a PMITP with intermittent feedstock feeding.

1. Introduction

Nanoparticles/nanopowder are expected as promising next generation material used in various applications such as in electronics, energy and environmental fields. Titanium dioxide (TiO_2) nanopowder is receiving attention as photocatalyst material, photonic crystals, photovoltaic cells, and gas sensors [1]–[4]. However, TiO_2 works as photocatalyst only under ultraviolet light because of its wide energy band gap. Attention has also been paid to TiO_2 nanopowder with metallic-ion doping as photocatalyst material. This is because the impurity energy levels in the band gap improve their visible light absorption efficiency [5]. Another application of metallic-ion doped TiO_2 is in the biomedical field [6]. It has been recently reported that Al-doped TiO_2 nanopowder has a protein-adsorption ability, which is effective to skincare for atopic dermatitis [7]. For biomedical applications, no contamination in TiO_2 or metallic-ion doped TiO_2 nanopowder is greatly desired. However, effective mass production methods have not yet been developed for such TiO_2 and metallic-ion doped TiO_2 nanopowder without contamination.

Various kinds of nanopowder synthesis methods have been developed so far. Among them, the inductively-coupled thermal plasma (ICTP) method offers great advantages [8]. For example, it can provide nanopowder with short processing time, and with simple one-step and continuous process. It can offer nanopowder in non-equilibrium or metastable phase. The most important feature of the ICTP method is that it can essentially synthesize nanopowder without

contamination due to the absence of electrodes. Many researchers have studied various kinds of nanopowder synthesis method using a steady-type of ICTP. However, nanopowder synthesis methods using steady-type ICTPs still have some issues such as the difficulty in controlling the synthesized particles size, and in the scale-up of the process for higher production rate [9]–[12].

The authors have developed a method to synthesize large amounts of nanopowder using the pulse modulated induction thermal plasma (PMITP) with time-controlled feeding of feedstock (TCFF), i.e. PMITP-TCFF method. The PMITP was developed to be controlled the time evolution of the temperature and reactive species fields in thermal plasmas using the coil current modulation. In addition to this, a method was also developed for feeding of feedstock powder. In this method, feedstock powder is intermittently and synchronously supplied with the coil current modulation of the PMITP. In our previous work, the PMITP-TCFF method was applied to synthesize pure TiO_2 and Al-doped TiO_2 nanopowder with large-scale production. Results indicated that this method using a 20 kW PMITP offered a high production rate of 500 g h^{-1} for pure TiO_2 nanopowder with a mean particle diameter around 43 nm, and 400 g h^{-1} for Al-doped TiO_2 nanopowder with a mean particle diameter around 67 nm [13, 14].

For a detailed understanding of this PMITP-TCFF method, it is important to study the evaporation process of the supplied feedstock powder and precursor production in gas phase for precise control of TiO_2 nanoparticle synthesis. This paper describes the two-dimensional spectroscopic observation of the PMITP-TCFF for TiO_2 nanopowder synthesis. For this purpose and experimental simplification, the feedstock feeding rate was intentionally adopted to be several g min^{-1} instead of several tens of g min^{-1}. The temporal-spatial variation for radiation intensities from some atomic spectral lines and molecular emission bands were measured during the coil current modulation and the intermittent feedstock powder injection. Finally, the evaporation of the feedstock powder and precursor formation processes are discussed from the obtained results.

2. PMITP-TCFF approach for large-scale nanopowder synthesis

The PMITP was developed to control the temperature and reactive species in the thermal plasma jet. The PMITP is sustained by the coil current modulated in a rectangular waveform. The PMITP has four control parameters: on-time, off-time, HCL and LCL. The 'on-time' is the duration of the higher current level (HCL) phase where a higher input power is supplied to the PMITP. In this 'on-time' temperatures in the plasma torch are higher. The 'off-time' represents the duration of the lower current level (LCL) phase where the input power to the PMITP is lower. During this phase, the plasma jet temperature is lower. In addition to these four parameters, we also defined a shimmer current level (SCL) and duty factor (DF). The SCL is the ratio of LCL to HCL, and the DF is the ratio of 'on-time' to a modulation cycle ('on-time'+ 'off-time'). The condition of 100%SCL or 100%DF corresponds to the non-modulation condition.

Figure 1 illustrates the comparison between two methods for nanopowder synthesis: One is the conventional method in which a steady type of ICTP (non-modulated ICTP) is used with continuous feedstock feeding, and the other is the PMITP-TCFF method. In the PMITP-TCFF method, a solenoid valve with a response time of 2 ms is installed on the feedstock feeding tube between the powder feeder and the PMITP torch. By switching the solenoid valve on and off, the feedstock is fed intermittently into the plasma torch intermittently and synchronously with the coil-current modulation. The feedstock is supplied into the plasma torch only during the high-temperature period. This intermittently and synchronously feedstock feeding can be executed by controlling the delay time t_d for opening the valve in reference to the pulse modulation signal of the PMITP coil-current. In the actual experiment, the feedstock reaches the PMITP torch in a finite time of t_{adt}. The t_{adt} was measured in our previous work as about 6-8 ms. Therefore, the actual delay time to the coil-current modulation signal is $(t_d + t_{adt}) \simeq (t_d + 7)$ ms.
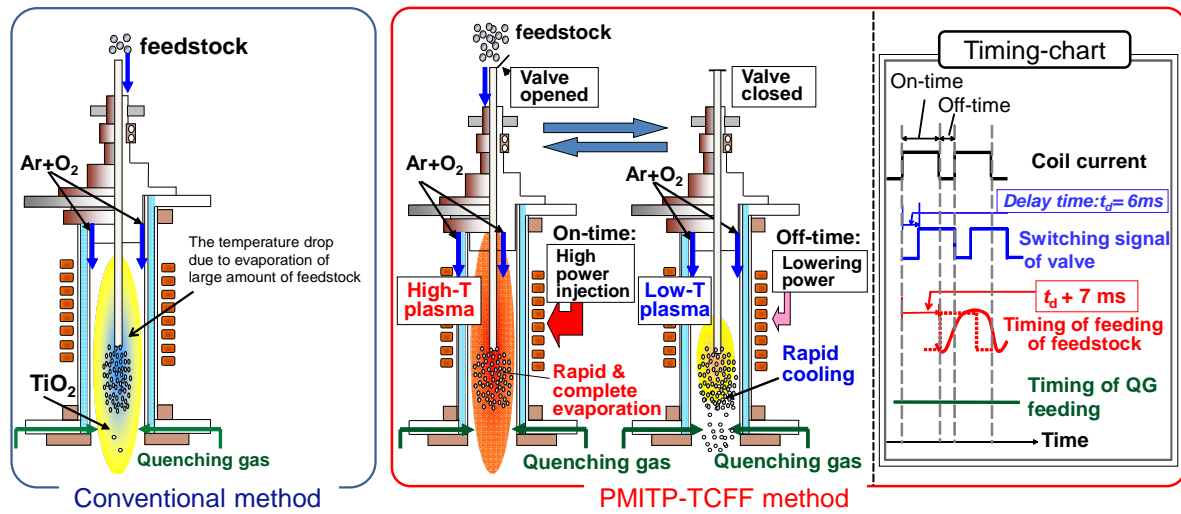
Figure 1. Method for large-scale nanopowder synthesis using induction thermal plasma. Left-hand side: conventional non-modulated ICTP with continuous feedstock feeding; Right-hand side: PMITP with intermittent feedstock feeding.

The injected feedstock is rapidly and completely evaporated during the high-temperature phase of the PMITP. The feedstock feeding is stopped by closing the solenoid valve during successive off-time. In the off-time, the evaporated feedstock material is rapidly and efficiently cooled down because the thermal plasma temperature decreases by the decreased input power to the PMITP. The evaporated Ti atom is mixed with Ar and O atoms from the thermal plasmas. The rapid cooling of the above atomic mixture promotes the nucleation of nanoparticles under the saturated vapor conditions. The nucleated nanoparticles are transported downstream of the PMITP while particle growth take place. The quenching gas (QG) injection downstream of the torch nozzle further cools the evaporated material to promote the nucleation of nanoparticles, thus restraining the particle growth. In this way, the PMITP-TCFF method enables the synthesis of nanopowder with a high production rate.

3. Experimental
3.1. Experimental conditions
The evaporation behavior of the powder injected in the PMITP-TCFF plasma torch is investigated. For comparison, we also measured the behavior for conventional non-modulated ICTP with continuous powder feeding, and for the PMITP with continuous powder feeding. Table 1 summarizes the experimental conditions. The plasma torch used is the same we used in our previous work[13, 14]. The total sheath gas flow rate was fixed at 100 l min^{-1}. The O_2/Ar gas admixture ratio was set at 10mol% in the sheath gas. The pressure in the chamber was regulated at 300 torr (=40 kPa). The quenching gas (QG) was not supplied in this work. The time-averaged input power was fixed at 20 kW. It is noted that instantaneous input power was changed periodically with time according to the coil current modulation. The modulation cycle was fixed at 15 ms. The DF of the modulated coil current was fixed at 80%. The SCL was set to two conditions: 100% (non-modulation condition) and 80%. The feedstock was Ti powder with a mean diameter of 27 μm (TILOP-45; Osaka Titanium Technologies Co.Ltd). The feedstock was fed into the thermal plasma using a rotary powder feeder with Ar carrier gas flow. The Ar carrier gas flow rate was fixed at 4 l min^{-1}. In the present experiments, the feeding rate of the feedstock was regulated at 4-7 g min^{-1}. This feed rate is much lower than what is
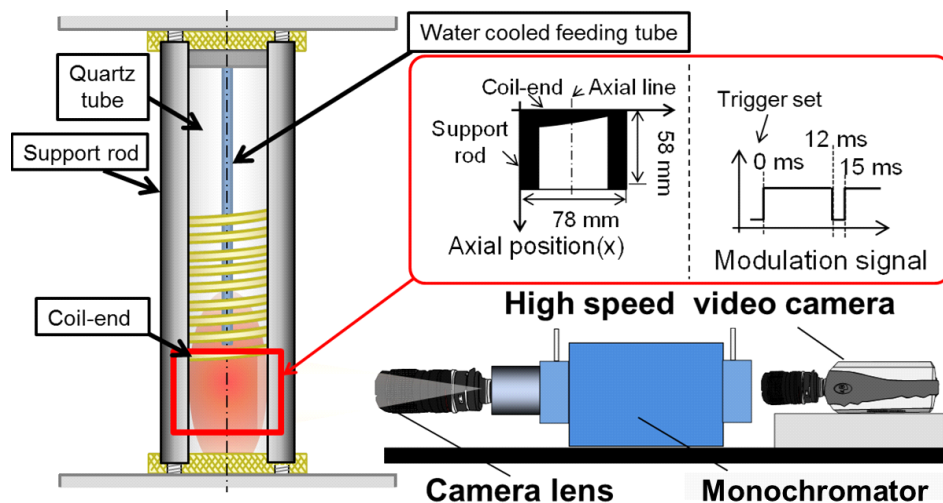
Figure 2. Spectroscopic observation system and observation area for an induction thermal plasma torch.

typically used for synthesis of large amounts of nanopowder [13, 14]. This small feed rate was adopted to carefully investigate the evaporation process. We set two feedstock feeding methods: the conventional continuous feeding and the intermittent feeding methods. The intermittent feedstock feeding was synchronized with the coil current modulation with a delay time t_{d} of 6 ms. The open and close time of the valve for the intermittent feedstock feeding were 12 ms and 3 ms, respectively. The powder was actually fed from the tip of the water-cooled feeding tube directly to the thermal plasma region. The tip of the water-cooled feeding tube was located between just above the coil end on the axis of the torch to allow spectroscopic observation.

3.2. Spectroscopic observation condition
Spectroscopic observation was carried out using a two-dimensional imaging spectrometry system(Anfi Inc., AN-IMC-DD) shown in figure 2. This system contains an objective lens (Nikon, AF Zoom-Nikkor 80-200 mm f/2.8D ED), a two-dimensional imaging spectrophotometer (Princeton Inst., Acton Spectra Pro 2300i), and a high speed video camera (NAC Imaging Tech., GX-8). The observation area was set to a 78×58 mm^2 region below the coil end. It is noted that the feedstock powder is supplied just above the coil end from the water-cooled feeding tube. The 1200 grooves/mm of diffraction grating was used for the spectrophotometer. In this case, the wavelength resolution of the spectrometer was 0.4 nm. This system can resolve time varying two-dimensional images at a selected wavelength using a high speed video camera. The atomic spectral lines of Ar I at a wavelength of 811.53 nm, O I at 777.54 nm were observed in the thermal plasma itself, and an atomic line of Ti I at 453.32 nm from the evaporated material. We also measured the molecular emission of TiO around 615.91 nm , which specie is formed by the chemical reaction of Ti + O. The frame rate of the high speed camera was set at 3000 fps.

4. Results and discussion
4.1. Synthesized nanoparticles
Figure 3 shows FE-SEM images of nanoparticles synthesized (a) by non-modulated ICTP (100%SCL) with continuous feedstock feeding , and (b) by PMITP (80%SCL) with intermittent feedstock feeding. As seen in figure 3, in both cases (a) and (b), many nanoparticles with diameters less than 100 nm were produced. The adopted feedstock feed rates being much

Table 1. Experimental conditions and spectroscopic observation conditions.

Time-averaged input power	20 kW
Fundamental frequency of the coil current	450 kHz
Modulation cycle	15 ms
Shimmer current level, SCL	100% (Non-modulation) or 80%
Duty factor, DF	80% (On-time / Off-time=12 ms / 3 ms)
Pressure	300 torr (= 40 kPa)
Gas composition	Ar:90 l min^{-1},O$_2$:10 l min^{-1}
Carrier gas flow rate	Ar:4 l min^{-1}
Quenching gas flow rate	None
Delay time of solenoid valve open t_{d}	6 ms
Feedstock feeding rate	4-7 g min^{-1}
Raw powder and its maximum size	Ti, 45 μm
Observation area	78×58 mm^2 region below the coil end
Wavelength resolution	0.4 nm
Spectral lines observed	Ar I (811.53 nm), O I (777.54 nm), Ti I (453.32 nm) and TiO (615.91 nm)
Frame rate for high speed video camera	3000 fps

(a)   (b)
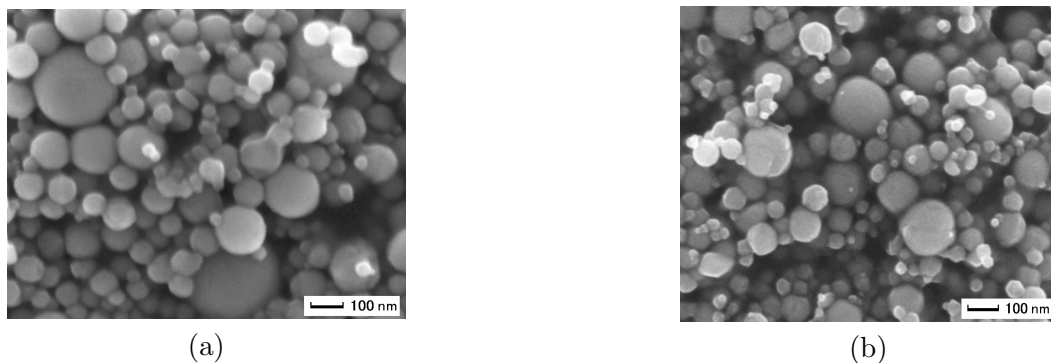
Figure 3. FE-SEM images of nanoparticles synthesized (a) by non-modulated ICTP, and (b) by PMITP with intermittent feedstock feeding (80%SCL)[15].

lower typical value used in synthesis of large-scale of nanoparticles [13, 14] , the feedstock was completely evaporated.

From randomly selected 200 particles in each of these FE-SEM images, the particle size distribution of synthesized particles were evaluated for different conditions. Figure 4 depicts the particle size distribution of nanoparticles synthesized (a) by non-modulated ICTP with continuous feedstock feeding, and (b) by PMITP with intermittent feedstock feeding (80%SCL). The mean particle diameter, and the standard deviation are also represented in figure 4. Nanoparticles with mean particle diameters around 55-65 nm were synthesized by the both methods even without quenching gas injection. In the next section, we focus an attention on
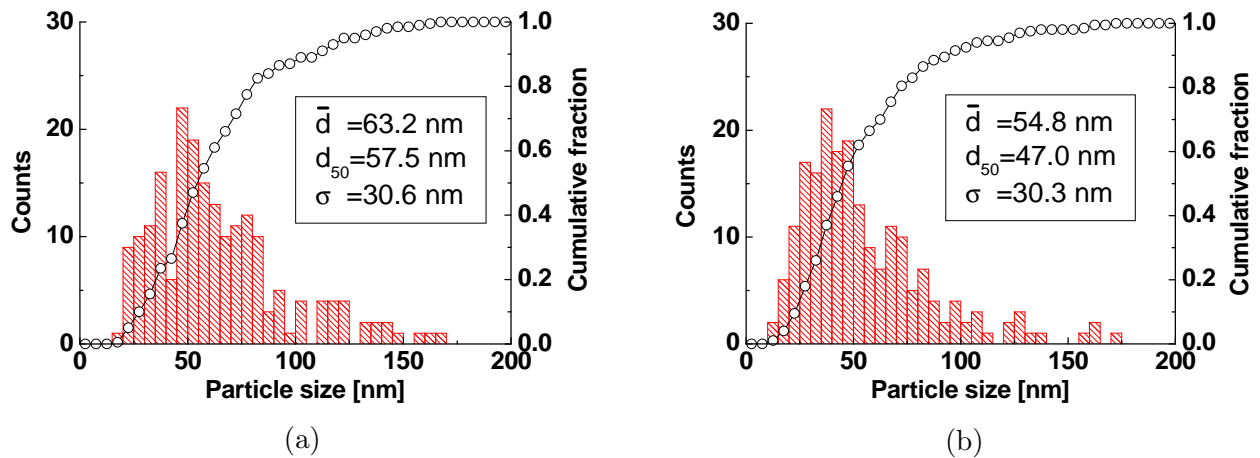
Figure 4. Particle size distribution of nanoparticles synthesized (a) by non-modulated ICTP and (b) by PMITP with intermittent feedstock feeding (80%SCL)[15].

the influence of the coil-current modulation and intermittent feedstock feeding on the feedstock evaporation process as well as the vapor cooling process.

4.2. Two-dimensional distribution of radiation intensities

Figures 5– 7 show temporal variations of the two-dimensional distribution of radiation intensities for (*a*) Ar I and (*b*) O I lines from the thermal plasma itself, that of (*c*) Ti I line from the evaporated material, and those of (*d*) TiO from by-product of Ti and O. In these figures, the timing *t* was also denoted at the bottom-left of each image. The coil current amplitude rises up at *t*= 0 ms, and falls down at *t* = 12 ms.

In case of the non-modulated ICTP with continuous feedstock feeding, the Ar I and O I radiation intensities were almost unchanged with time as shown in figures 5 (*a*) and (*b*). The Ar I and O I radiation intensities were almost uniform in the radial direction just below the coil end. However, the Ar I and O I radiation intensities decreased sharply downstream around the bottom of these figures, clearly indicating that the plasma tail of the ICTP is rapidly quenched. On the other hand, Ti atoms emit strongly around the axis, and especially in off-axis region below the coil end, as depicted in figure 5 (*c*). This implies that the injected Ti powder was evaporated by the thermal plasma to produce a high-density of Ti atoms, which were transported downstream. The Ti radiation intensity observed on the axis is lower than that in the fringe. This may be because the induction heating is present in the fringe, and the Ar carrier gas cools down the temperature on the axis. Figure 5 (*d*) presents the TiO spectral intensity distribution. The TiO is one important precursor for TiO_2 nanoparticle formation. The radiation intensity of TiO was detected locally on the axis. This means that TiO was formed in gas phase around the axis, and it transferred downstream by the Ar carrier gas flow.

Results for the PMITP with continuous feedstock feeding are presented in figure 6. The Ar I and O I lines had strong radiation intensities detectable from *t*=3–12 ms during the on-time, whereas these intensities became weaker in the off-time as shown in figures 6 (*a*) and (*b*). These results indicate that high and low temperature fields in the PMITP torch were repeatedly created with the coil-current modulation. Panel (*c*) indicates that Ti I radiation intensity from evaporated material was also varied with the coil-current modulation. The TiO radiation intensity were also detected on the axis with a peculiar time variation according to the coil-current modulation.

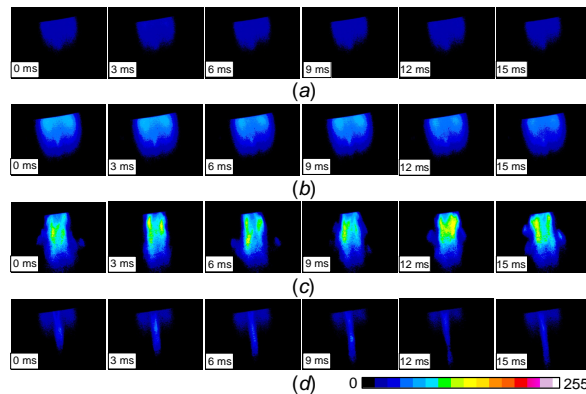The most important result is presented in figure 7 for the PMITP with intermittent feedstock

Figure 5. Two-dimensional distribution of radiation intensities for the non-modulated plasma (100%SCL) with continuous feedstock feeding. (*a*) Ar I: 811.53 nm, (*b*) O I: 777.54 nm, (*c*) Ti I: 453.32 nm, and (*d*) TiO: 615.91 nm.
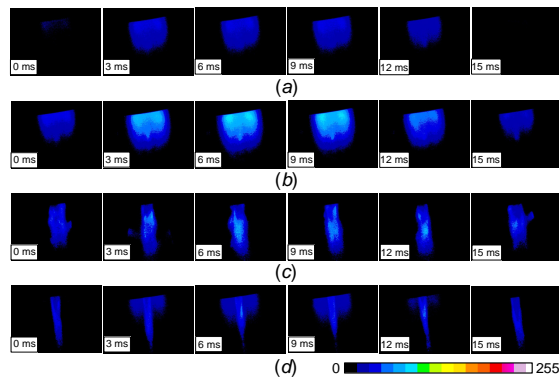

Figure 6. Two-dimensional distribution of radiation intensities from the PMITP for 80%SCL with continuous feedstock feeding. (*a*) Ar I: 811.53 nm, (*b*) O I: 777.54 nm, (*c*) Ti I: 453.32 nm, and (*d*) TiO: 615.91 nm.
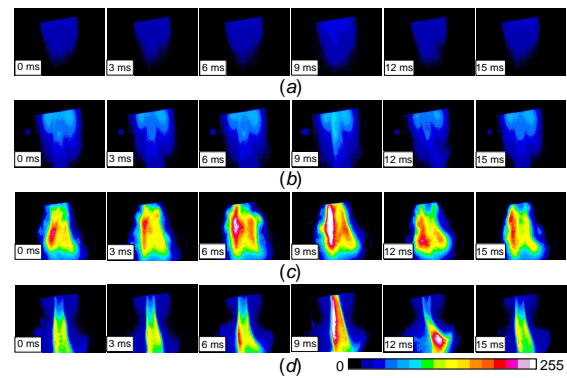

Figure 7. Two-dimensional distribution of radiation intensities from the PMITP for 80%SCL with intermittent feedstock feeding. (*a*) Ar I: 811.53 nm, (*b*) O I: 777.54 nm, (*c*) Ti I: 453.32 nm, and (*d*) TiO: 615.91 nm.

feeding. In this case, Ar I and O I radiation intensities similarly changed with the coil-current modulation. However, a large difference appears in Ti and TiO radiation intensities from those observed with continuous feedstock feeding. The radiation intensity of Ti I in intermittent feedstock feeding became much stronger than with continuous feedstock feeding. This is attributed to the fact that intermittent feedstock feeding has a higher instantaneous feeding rate during the on-time, and that the fed feedstock is efficiently evaporated by during the PMITP on-time. The Ti I radiation intensity depends on both Ti excitation temperature and Ti atomic density determined by evaporation amount of Ti feedstock. The result of the high Ti I intensity in panel (*c*) indicates that high-density Ti is present almost without a temperature drop even from feedstock loading because of high input-power to the PMITP during the on-time. In addition, the TiO intensity was strong just under the coil end. This result suggests that larger amounts of TiO was formed under the coil end region in this condition, and that it was transported downstream of the PMITP torch.
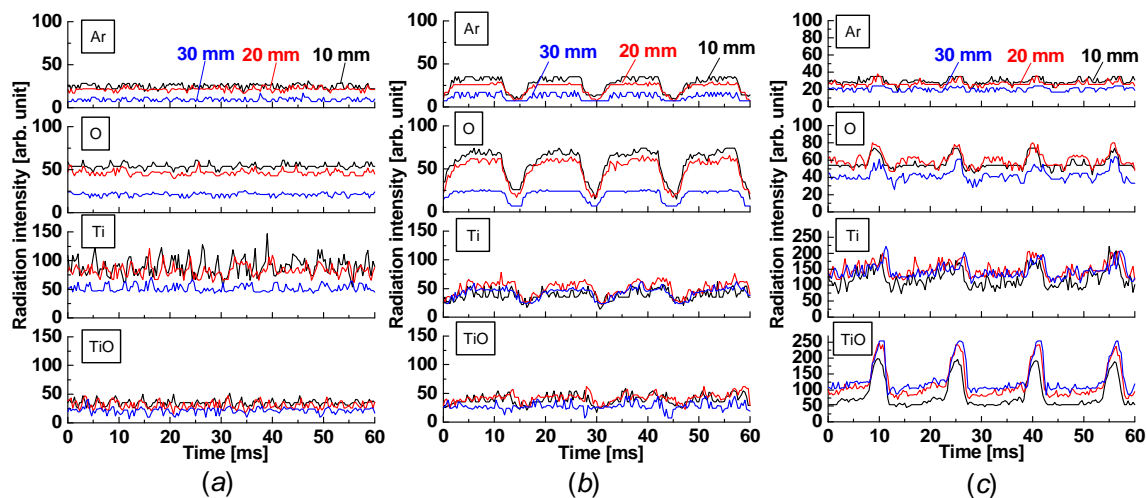
Figure 8. Temporal variation of radiation intensities of different spectral lines observed below the coil end. (*a*) Non-modulated coil current with continuous feedstock feeding, (*b*) modulated coil current of 80%SCL with continuous feedstock feeding, (*c*) modulated coil current of 80%SCL with intermittent feedstock feeding.

4.3. Temporal variation in radiation intensities for different spectral lines

Figure 8 illustrates the temporal variations in the radiation intensities of Ar I, O I, Ti I and TiO observed 10 mm, 20 mm and 30 mm below the coil end on the axis of the plasma torch. Panel (*a*) is the result for non-modulated coil current condition with continuous feedstock feeding; panel (*b*) is that for modulated coil current condition with continuous feedstock feeding, and panel (*c*) corresponds to the result for modulated coil current with intermittent feedstock feeding.

In case of non-modulation with continuous feedstock feeding, the Ar I and O I have almost unchanged radiation intensities, indicating stable sustainability of the thermal plasma torch. The radiation intensity of Ti I fluctuate due to the fluctuations in feedstock powder feeding and its evaporation. The TiO intensity is also hardly changed with time.

For modulated coil current with continuous feedstock feeding, the Ar I and O I radiation intensities periodically varied following the coil-current modulation. This result clearly shows that high-temperature and low-temperature fields in the PMITP torch were generated repeatedly. The radiation intensities from Ti I and TiO also change with time similarly.

A significantly different behavior of the time-varying radiation intensities for modulated coil current with intermittent feedstock feeding is observed. First, Ar I in the panel (*c*) has almost unchanged radiation intensity although the coil current was modulated. The O emission line intensity at 777.54 nm is almost constant similar to Ar I intensity except just before transition to the off-time. The radiation intensity of Ti I changes according to the pulse modulation but in almost triangular waveform. On the other hand, the TiO spectral intensity changes with time in periodical waveform, having a drastic increase just before transition to the off-time. We infer from those observations that the Ar I has almost unchanged intensity, which shows the unchanged plasma temperature in spite of the pulse modulation. This is inferred due to the energy balance between the increased input power by the coil current modulation and the increased loss power for evaporation of large amounts of feedstock during the on-time. The O emission line intensity increase just before transition to the off-time may be caused only by overlapping intensities from TiO band spectra around this wavelength because TiO band spectra has a wide wavelength region and high intensity in this case. The drastic increase in
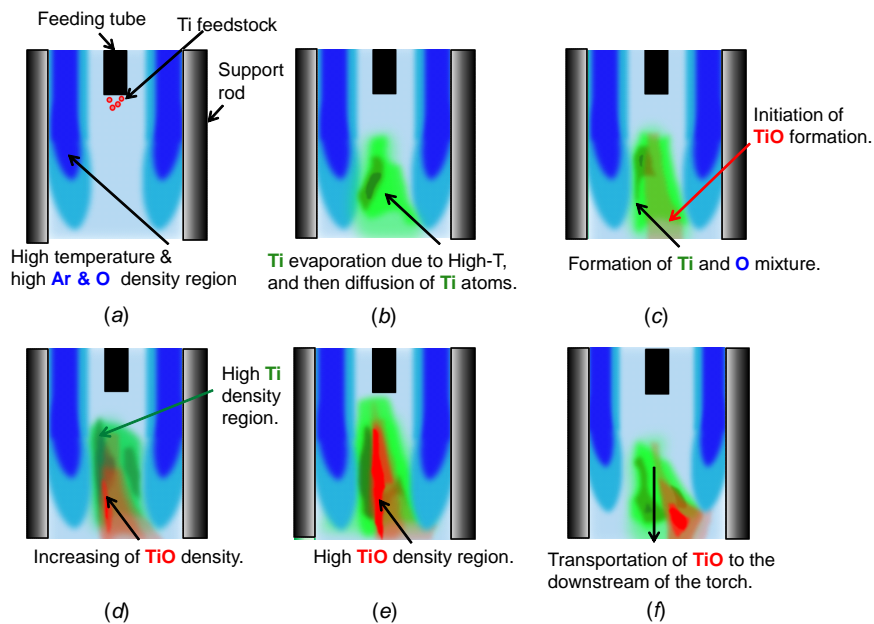
Figure 9. An interpretation on the evaporation process of Ti feedstock and the formation of TiO for pulse-modulation with intermittent feedstock feeding. (*a*) Input powder increase and initiation of feedstock feeding in on-time; (*b*) The evaporation of Ti feedstock, and then diffusion of Ti atoms in on-time (*t*= 0 ms); (*c*) Mixing of Ti and O atoms, and initiation of TiO formation around the axis (*t*= 3 ms); (*d*) Increasing of TiO density (*t*= 6 ms); (*e*) Formation of high TiO density region (*t*= 9 ms); (*f*) Transportation of TiO to the downstream of the PMITP torch (*t*= 12 ms).

TiO emission intensity may arise from a remarkable increase in TiO number density just before transition to the off-time. The remarkable increase in the TiO number density originates from promotion of formation reaction Ti + O → TiO because of Ti density increase from feedstock evaporation.

4.4. Discussion on Ti evaporation and TiO formation

The observations presented in the preceding sections lead to the following understanding of the evaporation process of Ti feedstock, formation of TiO, and the transport of TiO(precursor of TiO_2 nanoparticles). Figure 9 illustrates the schematic interpretation for phenomena happening in the plasma torch. The steps described as follows, where *t* is the time in figure 7:

(*a*) The Ti feedstock is supplied into the high-temperature thermal plasma just before the 'on-time' through the feeding tube. High Ar and O atomic density regions are present in off-axis region.

(*b*) At *t*= 0 ms, the coil current amplitude is increased to establish the high temperature thermal plasma. The Ti feedstock starts being evaporated to generate a high atomic density Ti region. Ti atoms in gas phase then diffuse in all directions.

(*c*) From *t*= 3 ms, a region containing Ti and O atoms is formed between the center-axis and the high-temperature region, and then TiO formation is initiated there.

(*d*) Around *t*= 6ms, TiO density increases with time around the center axis.

(*e*) Around *t*= 9 ms, further higher TiO density region is formed around the center axis.

(*f*) At *t*= 15 ms, TiO is transported downstream of the PMITP torch between off-time.

5. Conclusions

The two-dimensional distributions of spectral radiation intensities from pulse modulated induction thermal plasmas (PMITP) were investigated with continuous/intermittent feedstock feeding for TiO_2 nanopowder synthesis. For this measurement, an imaging spectrophotometer and a high speed video camera were adopted. The tempo-spatial distribution of radiation intensities for Ar I, O I, Ti I and TiO spectra were observed selectively. The observations provided spatial information on the evaporation of the Ti feedstock, mixing of Ti and O atoms, formation of TiO and the transport of TiO, i.e. the precursor of TiO_2 nanoparticles. This study dearly highlights the advantage of using the pulse modulation of the RF power and synchronous injection of feedstock over the conventional continuous process.

References

[1] Malato S, Blanco J, Alarcon D C, Maldonado M I, Fernandez-Ibanez P, and Gernjak W 2007 Photocatalytic decontamination and disinfection of water with solar collectors *Catalysis Today* **122** pp 137–49

[2] Li J, Zhao X, Wei H, Gu Z Z, and Lu Z 2008 Macroporous ordered titanium dioxide (TiO_2) inverse opal as a new label-free immunosensor. *Analytica Chemica Acta* **625** pp 63–9

[3] Gratzel M 2001 Photoelectrochemical cells. *Nature* **414** pp 338–44

[4] Biju K P and Jain M K 2008 Effect of crystallization on humidity sensing properties of sol-gel derived nanocrystalline TiO_2 thin films. *Thin Solid Films* **516** pp 2175–80

[5] Tsai Y C, Hsi C H, Bai H, Fan S K and Sun D H 2012 Single-step synthesis of Al-doped TiO_2 nanoparticles using non-transferred thermal plasma torch. *Jpn. J. Appl. Phys.* **51** 01AL01

[6] Lee K N, Kim Y, Lee C W and Jai-Sung Lee J S 2011 Simultaneous amination of TiO_2 nanoparticles in the gas phase synthesis for bio-medical applications *Mater. Sci. Eng.* **18** 082021

[7] Mio M, Kogoma M, Fukui H, and Kogoma A 2010 Control of inflammation using adsorption of inflammatory by nano-particles *Chem. Eng.* **55** pp 603-8

[8] Girshick S L, Chiu C P, Muno R, Wu C Y, Yang L, Singh S K, and McMurry P H 1993 Thermal plasma synthesis of ultrafine iron particles. *J. Aerosol Sci.* **24** pp 367–82

[9] Oh S M and Ishigaki T 2004 Preparation of pure rutile and anatase TiO_2 nanopowders using RF thermal plasma. *Thin Solid Films* **457** pp 186–91

[10] Tong L and Reddy R G 2006 Thermal plasma synthesis of SiC nano-powders/nano-fibers. *Materials Research Bulletin* **41** pp 2303–10

[11] Li J G, Ikeda M, Ye R, Moriyoshi Y, and Ishigaki T 2007 Control of particle size and phase formation of TiO_2 nanoparticles synthesized in RF induction plasma. *J. Phys. D: Appl. Phys.* **40** pp 2348–53

[12] Ishigaki T and Li J G 2007 Synthesis of functional nanocrystallites through reactive thermal plasma processing. *Sci. and Technol. Advanced Mater.* **8** pp 617–23

[13] Tanaka Y, Tsuke T, Guo W, Uesugi Y, Ishijima T, Watanabe S, and Nakamura K 2012 A large amount synthesis of nanopowder using modulated induction thermal plasmas synchronized with intermittent feeding of raw materials. *J. Phys. D: Conf. Ser.* **406** 012001

[14] Kodama N, Kita K, Tanaka Y, Uesugi Y, Ishijima T, Watanabe S, and Nakamura K 2014 A method for large-scale synthesis of Al-doped TiO_2 nanopowder using pulse-modulated induction thermal plasmas with time-controlled feedstock feeding. *J. Phys. D: Appl. Phys.* **47** 195304

[15] Tsuke T, Guo W, Tanaka Y, Uesugi Y, Ishijima T, Sakai Y, and Nakamura K 2012 The paper of Technical Meeting on Plasma Sci. & Technolo. IEE of Japan, PST-10-122